Article

A Portable Hybrid Photovoltaic Thermal Application: Shape-Stabilised Phase-Change Material with Metal Flakes for Enhanced Heat Transfer

Pakin Maneechot [1,*], Nivadee Klungsida [1], Thep Kueathaweekun [1], Narut Butploy [2], Sawet Somnugpong [2], Kanokwan Khiewwan [2], Jaturong Thongchai [2], Khumphicha Tantisantisom [3], Tholkappiyan Ramachandran [4,5], Madhan Kuppusamy [6,7] and Karthikeyan Velmurugan [8,9,*]

[1] Department of Energy, Faculty of Industrial Technology, Kamphaeng Phet Rajabhat University, Kamphaeng Phet 62000, Thailand; nivadee_k@kpru.ac.th (N.K.); thep_k@kpru.ac.th (T.K.)
[2] Department of Computer Technology, Faculty of Industrial Technology, Kamphaeng Phet Rajabhat University, Kamphaeng Phet 62000, Thailand; narut@kpru.ac.th (N.B.); sawet_s@kpru.ac.th (S.S.); kanokwan_kh@kpru.ac.th (K.K.); jaturong_t@kpru.ac.th (J.T.)
[3] Department of Information Technology, Faculty of Science and Technology, Kamphaeng Phet Rajabhat University, Kamphaeng Phet 62000, Thailand; khumphicha_t@kpru.ac.th
[4] Department of Physics, Khalifa University of Science and Technology, Abu Dhabi 127788, United Arab Emirates; tholkappiyan.ramachandran@ku.ac.ae
[5] Department of Physics, PSG Institute of Technology and Applied Research, Coimbatore 641062, India
[6] Department of Physics, Saveetha School of Engineering, Saveetha Institute of Medical and Technical Science, Saveetha University, Chennai 602105, India; mitmadhan@gmail.com
[7] GOONWORLD Corporate Research Institute, Daegu 11051, Republic of Korea
[8] Smart Energy System Integration Research Unit, Department of Physics, Faculty of Science, Naresuan University, Phitsanulok 65000, Thailand
[9] Department of Physics, Faculty of Science, Naresuan University, Phitsanulok 65000, Thailand
[*] Correspondence: pakin@kpru.ac.th (P.M.); karthi230407@gmail.com (K.V.)

Abstract: Photovoltaic–thermal (PVT) applications have been widely studied in recent years, though commercialisation has become critical due to their operational characteristics and size. In this study, a portable PVT system was developed for mobilisation with assistance from an organic phase-change material (PCM). Two different PCM composites were developed using the PCM with charcoal (PCM + C) and charcoal and metal flakes (PCM + C + M). Considering the portability of the PVT system, conventional metal-container-based PCM storage units were avoided, and the shape-stabilised PCMs (SS-PCMs) were fitted directly on the back surface of the PV module. Further, a serpentine copper tube was placed on the SS-PCMs to extract heat energy for hot water applications. It was found that $PV_{PCM+C+M}$ exhibited a higher cooling rate, with peak reductions of 24.82 °C and 4.19 °C compared to the PV_{noPCM} and PV_{PCM+C}, respectively. However, PV_{PCM+C} exhibited a higher outlet water temperature difference of 11.62 °C. Secondly, an increase of more than 0.2 litres per minute showed a declining trend in cooling in the PV module. Considering the primary concern of electrical power generation, it was concluded that $PV_{PCM+C+M}$ is suitable for PVT mobilisation applications, owing to it having shown the highest thermal cooling per 190 g of PCM and a 1-Watt (TCPW) cooling effect of 2.482 °C. In comparison, PV_{PCM+C} achieved a TCPW cooling effect of 1.399 °C.

Keywords: hybrid application; shape-stabilised PCM; metal flakes; efficiency enhancement

1. Introduction

In modernised society, energy consumption has become vital, and most conventional energy generators rely on fossil fuels. Environmental pollution is mainly attributed to the vast usage of fossil fuels, resulting in major cities in Thailand, like Bangkok and Chiang Mai, facing high levels of $PM_{2.5}$, which complicates the routine life of infants and older people [1,2]. The Ministry of Energy in Thailand and the Electricity Generating Authority of Thailand (EGAT) encourage renewable energy systems to reduce environmental pollution and fossil fuel consumption. Thailand, a tropical country with more than 300 days of effective sunshine yearly, can favour solar-based energy generation [3,4]. Most renewable energy systems generate electrical or thermal power, but only in solar energy systems can both electrical and thermal power be obtained separately and in combination [5,6]. In this study, photovoltaic–thermal (PVT) applications are reviewed as eco-friendly, cost-effective solutions for electrical and thermal power requirements. A solar photovoltaic system converts photons into electrical energy by the photovoltaic effect. During the electrical energy conversion process, 18–25% of fallen sunlight is typically converted into electrical energy, and the rest is absorbed as heat energy. The accumulation of heat energy in the PV module causes a voltage drop, which reduces overall power production. Secondly, operating the PV module under thermal stress could lead to material degradation over a long time. Removing the heat energy from the PV module increases the module's efficiency, and utilising the excess heat for thermal applications minimises the conventional thermal load [7–9].

Recovering the waste heat from PV module surfaces has been widely performed in the last several decades using thermal collectors attached to PV modules' rear surfaces [10,11]. Integrating the heat tubes directly on a PV module's Tedlar surface can break the structure of the PV module, and heat recovery cannot be effective due to the low thermal conductivity of the Tedlar surface [12]. High-thermal-conductivity metals are placed between the PV module and the heat tubes for improved heat recovery, and the heat pipes can easily absorb the heat energy from the PV module [13,14]. A constant water flow inside the heat tubes can remove the heat and deliver hot water; PV modules are cooled during this process [15,16]. Though the thermal collectors remove the higher heat energy, they fail to achieve a higher cooling effect for the PV module due to uneven heat transfer. With the advancement of PVT collectors, phase-change materials (PCMs) have been used to improve heat transfer and stabilise the cooling and heating effects of PV modules and water, respectively [17,18]. Elsheniti et al. developed a PCM-assisted PVT thermal collector and experimented with desert climatic conditions. PCM blocks were attached to a heat pipe for distributed and stabilised heat transfer. To maintain the water pressure within the heat pipe, the inlet and outlets were positioned on the header side of the PV module. The six-day experimental study revealed that the cooling effects were high during the peak sunshine hours; beneficially, the developed cooling system achieved a 3.2 °C PV-module temperature (T_{PV}) reduction on average. This decrease in T_{PV} greatly enhanced the electrical, thermal, and combined efficiency to 10.34%, 71.16%, and 81.5%, respectively [19]. Though the PCM is an excellent thermal energy storage material, it removes the heat from the PV module during the PCM melting state, as it initiates the latent heat property. If the PCM fails to reach its latent heat property in an effective sunshine period, the cooling effect can be adverse to the unmodified PV module or lower, and no cooling effect can be achieved. Several studies have reported that the primary issue in cooling a PV module using PCM is finding an appropriate melting temperature [20–22].

Elarga et al. examined three locations using RT42 (Venice, Italy, and Helsinki, Finland) and RT55 (Abu Dhabi, United Arab Emirates). Considering the weather patterns of Venice and Helsinki, low melting temperatures were chosen compared to Abu Dhabi. In Venice, a

peak T_{PV} reduction of 10 °C was achieved. The same PCM operated differently in Helsinki due to strong irradiance in summer, causing a higher T_{PV} for the conventional systems and elevated air circulation in the PV module's front and the PCM's back surface cavity, which favoured a cooling maximum of 20 °C. Under high ambient temperatures, RT55 is regulated at a maximum of 17 °C. The required melting temperature for the selected location had to be obtained to regulate the PV module's operating temperature [23]. The operation of a PCM in cooling a PV module differs between passive and active methods. For passive methods, if the melting temperature is higher/lower than the required range, ineffective cooling will be achieved. Comparatively, active methods can effectively cool the PV module using slightly lower melting temperatures, as the active fluid flow allows the PCM to operate under a mushy state for longer. However, selecting a higher melting temperature will face similar issues to passive methods.

The second major concern about PVT-PCM was the low thermal conductivity property, which restricted heat extraction from the PV module and from the PCM to the heat pipe [24,25]. Integrating thermal fins inside the PCM container was a complex design. To overcome this issue, PCM with a finned container was split into 20 segments, where it could be easily installed and had a maintenance-free system design. Under real-time operating conditions in Colombia, an RT35 commercial PCM reduced the PV module temperature (T_{PV}) by a maximum of 17 °C during the peak sunshine hours. The average electrical efficiencies of the unmodified PV and PVT-PCM attained 13.12% and 14.14%, respectively, while the thermal and hybrid efficiencies of the PVT-PCM were 17.33% and 31.35%, respectively [26]. Bassam et al. developed a micro fin tube-assisted thermal collector and a silicon carbide-based nano-PCM. The study was performed in controlled environmental conditions with 600 W/m^2, 800 W/m^2, and 1000 W/m^2; the inlet water temperature was maintained at 18 °C with a different flow rate ranging from 0.5 to 2.5 L/min (LPM). Under steady-state conditions, the nano-PCM with a micro-finned tube and water as the working fluid reduced the T_{PV} by a maximum of 41.6 °C. Within the same environmental conditions, nanofluid as a working fluid enhanced the cooling effect by 3.2 °C compared to water as the working fluid [27]. Apart from the composite PCM, paraffin wax with a melting temperature of 57 °C enhanced higher cooling with the help of thermal conductivity-enhanced heat transfer fluid (HTF). A multi-wall carbon nanotube (MWCNT) with 0.2% water as a HTF attained higher PV module cooling of 12.18 °C, whereas 50% ethylene glycol with water attained lower T_{PV} reduction than pure water [28].

It is well known that PCM undergoes phase during the charging and discharging of thermal energy. Conventionally, filling PCM in a container can lead to high pressure during the liquid phase, resulting in leakage. To prevent liquid PCM leakage, Emam et al. encapsulated RT35 commercial PCM into copper spherical balls, using 22 units, and placed them on the back surface of the PV module. A constant water flow rate of 2 LPM was maintained through the PCM sphere balls in the thermal energy storage chamber to cool both the PV module and the PCM balls. A year-round PV module cooling study revealed that the highest and lowest cooling effects were observed in July and November, with average temperature differences of 4.14 °C and 1.86 °C, respectively. However, a higher electrical efficiency of 16% was achieved in June due to the early summer period, characterised by elevated ambient temperatures and clear sunshine. In terms of thermal efficiency, the summer months of June, July, and August achieved values of 46%, 53%, and 46%, respectively, which were higher than those of other months [29]. Almeshaal and Altohany developed a PCM container using two different materials. The top surface of the PCM container was fabricated from a copper sheet, while the remaining sides were made of acrylic glass. RT35 commercial PCM was encapsulated within copper spheres, each with a diameter of 50 mm and a wall thickness of 2 mm. The encapsulated PCM spheres were

placed inside the PCM container in physical contact with the copper sheet, while water or CuO-based heat transfer fluid (HTF) flowed through the PCM container between the 20 PCM spheres. A water flow rate of 0.5 LPM significantly enhanced cooling, reducing the T_{PV} by up to 6.18 °C. Notably, increasing the water flow rate to 1 LPM and 1.5 LPM resulted in additional cooling of 0.42 °C and 1.32 °C, respectively, compared to the 0.5 LPM flow rate. Furthermore, flow rates of 1 LPM and 1.5 LPM were used to analyse different ratios of CuO in the HTF. Increasing the CuO ratio reduced the cooling effect from 10.2 °C to 9.2 °C; however, the CuO-based HTF still provided greater cooling compared to pure water [16].

The above literature and Table 1 demonstrate that PCM is an excellent thermal energy storage material, offering a sharp charging point at a desired temperature and a high latent heat of fusion. However, integrating PCM with PVT collectors encounters several operational challenges, primarily low thermal conductivity and liquid PCM leakage. Beyond these operational characteristics, PVT-PCM systems have failed to achieve commercial viability due to their bulk nature, fabrication complexity, and high cost. To address these challenges, this study incorporates locally available charcoal composited with lauric acid (LA) to prevent liquid PCM leakage. Additionally, aluminium metal flakes are added to enhance the thermal conductivity of the shape-stabilised PCM. The shape-stabilised and thermal conductivity-enhanced PCMs are directly applied to the Tedlar surface, eliminating the need for a bulky structure. To achieve a compact and portable PVT-PCM system, a 1.5 cm thick layer of PCM is utilised, fitting seamlessly within the frame of the PV module structure and incorporating a heat pipe inside the PCM.

Table 1. Recent literature on PVT-PCM technical parameters.

Location	PV (W)	PCM	Fluid Type	Tube Size (mm)	Tube Type	HTF Flow Rate	PCM Container (kg/Thickness)	Reference
Iran	80	Paraffin wax = 57–60 °C	Water, MWCNT, ethylene glycol	8	Cu	30–50 LPH	2 kg	[28]
China	-	Paraffin wax = 32.42 °C	Water	10	Cu	500–750 LPH	-	[30]
Colombia	310	RT35	Water	10	Cu	36 LPH	11.05 kg/ 2.5 cm	[26]
China	40	Paraffin wax = 46, 2.5 cm	Water	10	Cu	20–60 LPH	2 kg	[31]
Iran	40	Paraffin wax = 46 °C	Water	10	Cu	30 LPH	2 kg	[32]
India	-	noPCM	Water	6.25	Cu	36 LPH		[33]
China	17	TH-SL35 = 37 °C	Water	5.5	Cu	102 LPH	12.6 kg	[34]
China	135	PCM = 15 °C	Water	10	Cu	-	2.6 cm	[35]
China (Indoor)	100	Capric acid = 30.1 °C	Water	8	Cu	150 LPH	5.27 cm	[36]
India	100	RT 30	Water	12.7	Cu	47–112 LPH	65 kg	[37]
India	100	OM42	Water	8	Cu	29.8 LPH	3.68 cm	[38]
Egypt	10	RT35	Water	6.35	Cu	48–96 LPH	8 kg	[39]
Poland	10	Paraffin wax = 42–44 °C	Water	-	-	32–80 LPH	2–4 cm	[40]
France	110	OM 37	Water	-	Cu	144	50 kg	[41]
Turkey	40	RT55	Water	7	Cu	60 LPH	2 kg	[42]
Thailand	10	LA	Water	6	Cu	0.2, 0.4, 0.6, 0.8 LPM	190 g, 280 g	Present study

2. Materials and Methods

Thailand is a tropical country rich in solar potential, contributing up to 34% of national renewable energy generation, depending on solar PV systems [43]. However, the high solar irradiance and ambient temperatures cause solar farms to experience severe thermal stress, adversely affecting their performance and longevity [2]. Several studies have indicated that cooling the operating temperature of PV modules using PCM can significantly enhance system performance. To effectively use PCM as an auxiliary system to cool the PV module temperature, it is necessary to consider suitable thermophysical properties, including selecting an appropriate melting temperature for the PCM. If the PCM fails to reach its latent heat state, it will not be effective in controlling the PV module's operating temperature. Based on the existing PV module cooling techniques, it is important to perform the cooling operation with organic PCMs, particularly those with a melting temperature of less than 45 °C [21,22,44]. In this study, lauric acid (LA) is selected due to its sharp melting temperature of 42.3 °C, high latent heat of fusion of 187 J/g, and thermal stability for extended operation with negligible volume expansion, as listed in Table 2 [45]. Furthermore, it melts congruently, is chemically stable, less corrosive than salt hydrates, is suitable for large-scale implementation, and is lower in cost compared to commercial and inorganic PCMs [46].

Table 2. Thermophysical properties of lauric acid (LA) [45].

PCM	Melting Temperature (°C)	Latent Heat of Fusion (J/g)
Lauric Acid	42.3	187

2.1. Preparation of PCM

Lauric acid (LA), with a purity of 99%, was purchased from Tree Shade Co Ltd., Bangkok, Thailand, and its thermophysical properties are listed in Table 2 [45]. The charcoal was purchased from a local shop, while aluminium metal flakes (1100) were collected from industrial scrap, with a maximum length of 20 mm. PCM + Charcoal (PCM + C): Without further chemical treatment, 280 g of LA was melted and maintained at 80 °C for compositing with 170 g of ground charcoal (60.71:39.28 wt.%). The composite materials were kept at 80 °C for 4 h to ensure effective PCM impregnation and prevent leakage. Subsequently, the composited PCM was cooled to ambient temperature and grated into flakes with a maximum length of 15 mm, making it easy to integrate with the PV module's Tedlar surface and heat pipes. PCM + Charcoal + Metalflakes (PCM + C + M): The same procedure was followed for compositing LA and charcoal; however, the material proportions were adjusted to 190 g (42.22 wt.%) of LA and 130 g (28.89 wt.%) of charcoal. Although charcoal serves as both a shape stabiliser and a thermal conductivity enhancer, aluminium metal flakes were added as a secondary thermal conductivity enhancer. A total of 130 g (28.89 wt.%) of aluminium metal flakes were mixed with the prepared composite PCM flakes.

2.2. Experimental Setup

This study employs three 10 W polycrystalline PV modules. The first unmodified module serves as a reference PV module (PVnoPCM). The second PV module was integrated with charcoal and LA, while the third incorporated charcoal, metal flakes, and LA. Both PV modules are equipped with a 450 g thermal energy storage unit, through which a serpentine heat transfer pipe passes through the shape-stabilised PCM, as shown in Figure 1a. The technical parameters of the PV modules and thermal energy storage units are detailed in Table 3. The grated shape-stabilised PCMs were applied to the PV module's Tedlar surface with a thickness of 1.5 cm, and the backside of the PCM was enclosed with a 5 mm acrylic

glass layer. While increasing the thickness of the PCM would enhance the cooling effect, it poses challenges such as added weight, handling difficulties, and increased cost, making it unsuitable for commercial applications. Additionally, active cooling systems with a water flow inside the PCM unit do not necessitate more heat storage capabilities than passive cooling techniques. However, a 1.5 cm thickness of PCM without fluid motion could have adverse effects on cooling the PV module, especially when composited with charcoal. This study primarily focused on the active cooling system. Furthermore, this study aimed to perform the PV module cooling process using a minimal amount of PCM. For this purpose, a 1.5 cm PCM layer was integrated onto the Tedlar surface, which fits within the PV module frame without requiring additional modification to the PV/PCM unit and allows smooth enclosure using acrylic glass.

Table 3. Technical parameters of the PV module and thermal energy storage system collector.

Parameters	Range
PV module	
Power	10 W
Open circuit voltage (Voc)	21.6 V
Short circuit current (Isc)	0.57 A
Voltage at maximum power (Vmp)	18 V
Current at maximum power (Imp)	0.55 A
Thermal energy storage collector	
PCM Surface area (L $\times$ W $\times$ D)	23 $\times$ 34 $\times$ 1.5 cm
Heat transfer tube inner diameter	0.4 cm
Heat transfer tube outer diameter	0.6 cm
Acrylic glass thickness	0.5 cm
PCM thickness	1.5 cm

All three PV modules were mounted at a fixed tilt angle of 16○, and the experiments were conducted at Kamphaeng Phet Rajabhat University (KPRU), Thailand. The experiments were carried out during October and December, transitional periods between the monsoon and winter seasons, when hot water demand typically increases. K-type thermocouples were employed to measure the PV module temperature, PCM backside surface temperature (acrylic), ambient temperature, water inlet temperature, and water outlet temperature, as shown in Figure 1b. The solar irradiance was collected from the zero-energy building at the energy park (KPRU). Temperatures and solar irradiance were recorded at one-minute intervals using a data logging system, while the electrical output of the PV modules was measured every 60 min. The PV module's maximum voltage and current were manually measured using a variable resistance.
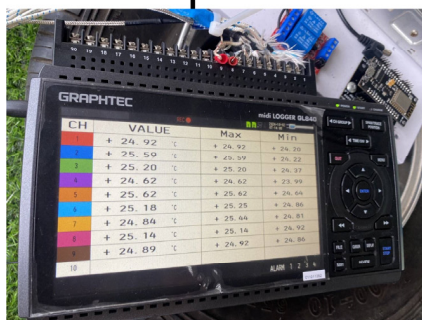
PV with heat transferring pipe

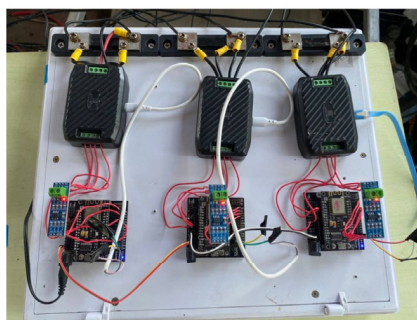PV with heat transferring pipe
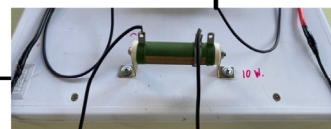and PCM+charcoal+metalflakes

Magnified observation of metal
flakes

(**a**)

Pyranometer

PV_{noPCM}   PV_{PCM-C}   PV_{PCM+C+M}

Variable Resistive Load

Data Acquisition System 1   Data Acquisition System 2

(**b**)

Figure 1. Schematic view of (**a**) the thermal energy storage system and (**b**) real-time experimental operating conditions.

3. Heat Transfer Mechanism

Figure 2 shows the heat transfer mechanism of the developed system compared with an uncooled PV module. The left-hand side (PV$_{noPCM}$) represents the heat transfer network of a PV module operating without an external cooling agent. Typically, the front surface of the PV module (solar glass) naturally dissipates heat energy to the surroundings and the sky, which is generated during the power conversion process. Depending on the airflow over the flat surface of the PV module, heat dissipation to the ambient environment occurs via natural convection (R$_{AMB}$). Additionally, with or without the temperature difference between the PV module's front surface and the surroundings, heat is dissipated to the sky through radiative heat transfer (R$_{SKY}$). Although heat energy is naturally ventilated, the PV module operates under significant thermal stress due to elevated ambient temperatures and a lack of consistent wind speed. The back surface of the PV module also dissipates heat using the same methods as the front surface; however, the back surface encounters higher resistance to heat dissipation.
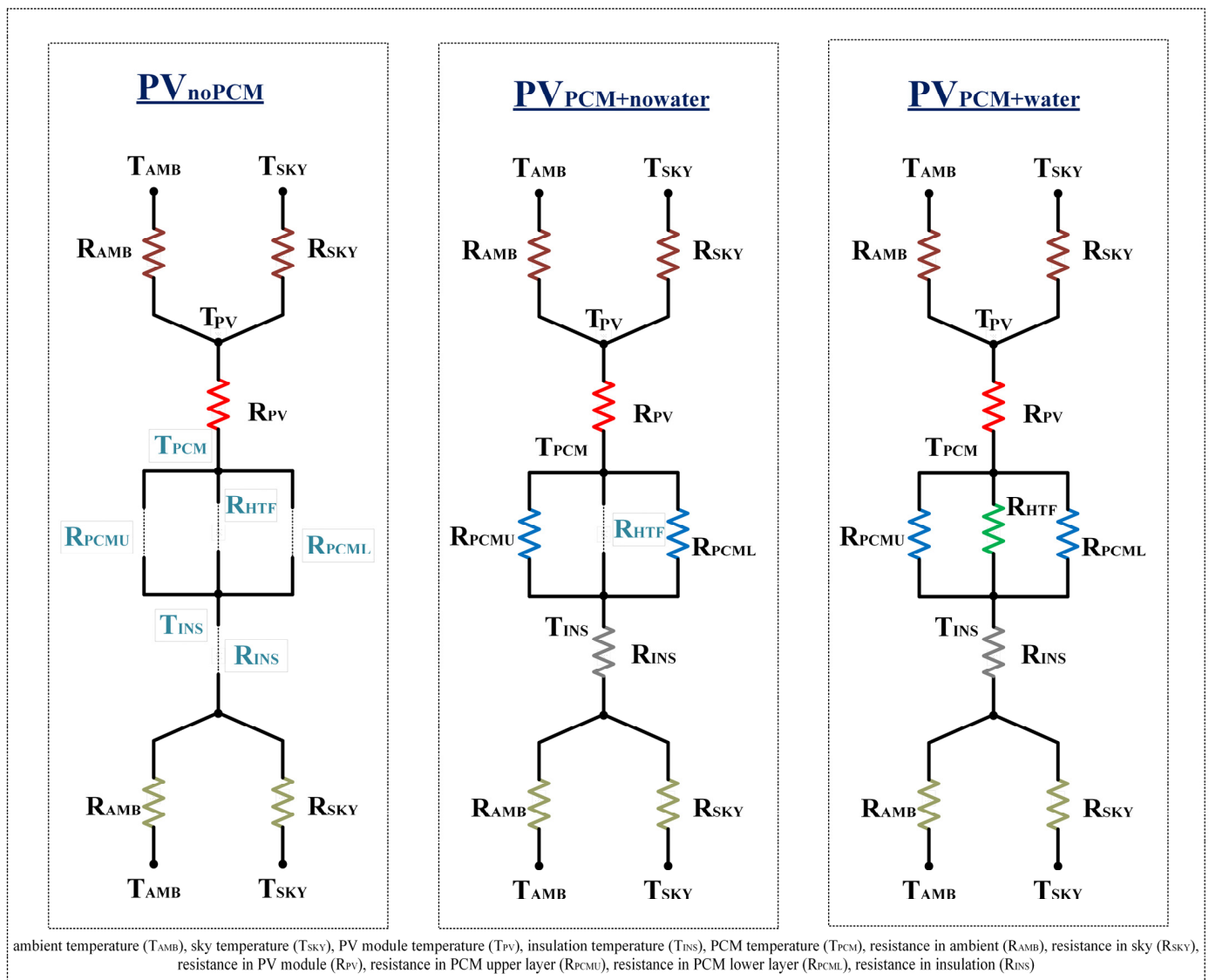

ambient temperature (T$_{AMB}$), sky temperature (T$_{SKY}$), PV module temperature (T$_{PV}$), insulation temperature (T$_{INS}$), PCM temperature (T$_{PCM}$), resistance in ambient (R$_{AMB}$), resistance in sky (R$_{SKY}$), resistance in PV module (R$_{PV}$), resistance in PCM upper layer (R$_{PCMU}$), resistance in PCM lower layer (R$_{PCML}$), resistance in insulation (R$_{INS}$)

Figure 2. Heat transfer mechanism of PVnoPCM, PVPCM without and with water flow.

In most cases, radiative heat transfer to the ground is negatively impacted due to reflection from the ground. Moreover, the ground absorbs solar energy stored during the day and releases it as heat, resulting in elevated ambient temperatures that do not

decrease proportionally to the decline in solar irradiance. This delayed heat release from the ground creates additional thermal resistance, hindering effective cooling. The increased thermal resistance beneath the PV module suppresses the convection processes because wind circulation beneath the PV module is less effective than at the front surface. These factors contributed to elevated PV module operating temperatures in tropical regions. To address these issues and improve system efficiency, a PCM unit was attached to the back surface of the PV module. To investigate the heat transfer behaviour of the developed system, cooling operations using PCM without water flow were performed under real-time operating conditions. The PCM-integrated PV module is equipped with thermal insulation on the back surface of the acrylic glass to minimise heat loss from the PCM. The heat extracted from the PV module is intended for hot water production; however, in the absence of water flow, no hot water is produced, even with the insulation in place. This indicates that heat dissipation is effectively controlled at the system's back surface. The right-hand side ($PV_{PCM+water}$) in Figure 2 represents the heat transfer mechanism of the developed system. A constant water flow rate through the PCM unit maintains the PCM in a mushy state, facilitating effective cooling of the PV module.

4. Results and Discussions

4.1. Thermal Analysis of PV Module with Shape-Stabilised PCM

4.1.1. Without Water Flow

PCMs are well-known thermal energy storage materials that utilise latent heat of fusion during phase transitions. Integrating a PCM unit behind a PV module enhances cooling and power generation. In hybrid PV and thermal applications, PCMs are insulated to minimise heat loss, which can otherwise negatively affect PV module performance under certain conditions. To evaluate the potential negative impact of integrating a PCM unit with a PV module, a no-water-flow analysis was performed under real-time operating conditions. Peak and average solar irradiances of 799.7 W/m^2 and 482.67 W/m^2, respectively, were observed, as shown in Figure 3. As solar irradiance increased, the ambient temperature rose to an average of 34.7 °C, resulting in a rise in the PV module operating temperature, which peaked at 68.4 °C and averaged 51 °C. The PCM + C configuration assisted the PV module in maintaining a lower operating temperature until 09:30. However, further increases in solar irradiance revealed a negative impact on the cooling performance, as the PCM failed to enhance heat transfer between the PV module and the PCM unit. This failure to cool the PV module can primarily be attributed to the thickness of the PCM unit, which was 1.5 cm. Additionally, insulating the PCM unit's backside created resistance to heat dissipation. Furthermore, the absence of fluid motion caused the PCM temperature to rise more rapidly, preventing the latent heat of fusion from being effectively utilised for cooling the PV module. In comparison, the PCM + C + M configuration resulted in a higher PV module temperature than PV_{noPCM} throughout the experimental period due to the lower mass composition of PCM in this setup. Both the PCM + C and PCM + C + M back surfaces reached the PCM melting temperature at 09:47, indicating the end of the latent heat storage phase. After this point, the cooling effect of the PCM + C became less effective than PV_{noPCM}. Within 125 min of the experimentation period, the latent heat of fusion was completely utilised, and the PCM reached the end of its melting phase at 10:05. The PV_{noPCM} configuration attained peak and average operating temperatures of 68.38 °C and 50.97 °C, respectively. In contrast, the PCM + C recorded peak and average temperatures of 72.79 °C and 56.01 °C, while the PCM + C + M exhibited the highest temperatures at 85.61 °C and 64.27 °C, respectively. These results highlight that a lower PCM thickness, combined with insulation, can have adverse effects on the cooling performance. However, the no-water-flow condition was performed to understand the thermal behaviour of the

developed system under passive conditions. The impact of varying water flow rates on the system is explored in the following subsection.
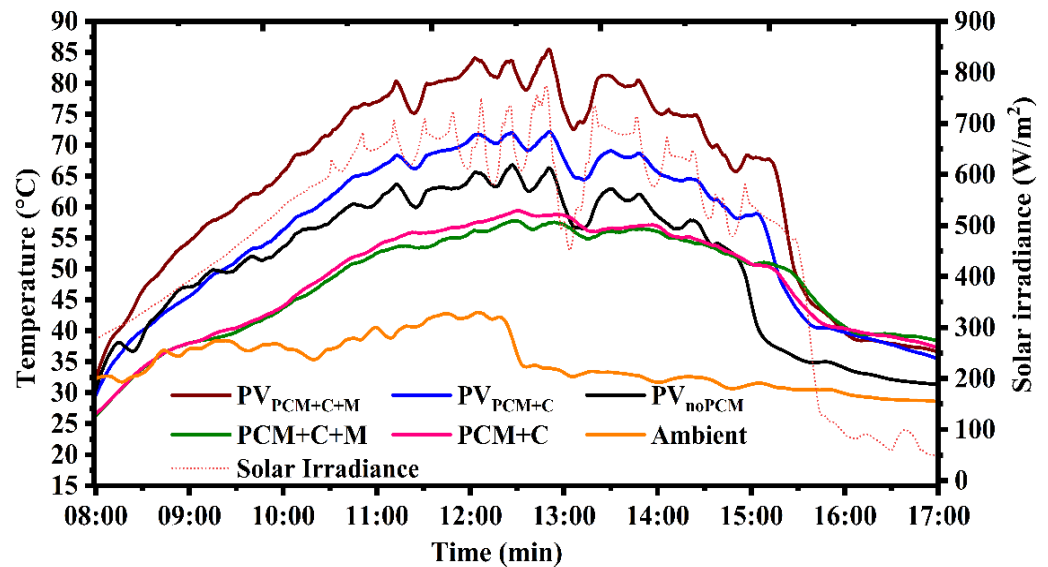

Figure 3. Meteorological and thermal profiles of PV_{noPCM}, PV_{PCM+C}, and $PV_{PCM+C+M}$.

4.1.2. Water Flow at 0.2 LPM

Figure 4a shows the PV module operating temperature and solar irradiance trend at a constant water flow rate of 0.2 LPM. The presence of 0.2 LPM of water flow inside the PCM unit enhances heat transfer between the PV module and the PCM, resulting in maximum temperature reductions of 24.82 °C and 20.63 °C for PCM + C- and PCM + C + M-assisted PV modules, respectively. On the experimental day, the average operating temperatures of the PV_{noPCM}, PV_{PCM+C}, and $PV_{PCM+C+M}$ configurations were 52.26 °C, 43.19 °C and 41.84 °C, demonstrating the effectiveness of the PCMs in improving the cooling performance. The water flow within the PCM unit helps maintain the latent heat of fusion storage property over an extended period. Although a constant water flow rate of 0.2 LPM was applied to both PCM units, the backside of the PCM + C reached a higher temperature of 45.48 °C due to its lower thermal conductivity and the high proportion of PCM composited with charcoal, as shown in Figure 4b. However, this temperature increase resulted in only a minor variation in the cooling performance of the PV module, with an average temperature difference of 1.35 °C compared to the PCM + C + M configuration. Both PCMs effectively utilised their latent heat of fusion throughout the experimentation period, keeping the PV module temperatures lower than those of the PV_{noPCM} configuration. A slight temperature oscillation was observed in the PCM + C + M-assisted PV module between 10:30 and 12:00, attributed to the lower mass fraction of PCM. A sudden increase in solar irradiance caused an abrupt rise in the PV module temperature, making it challenging for the PCM to dissipate the additional heat energy, particularly in the PCM + C + M configuration compared to the PCM + C. Due to the higher temperature of the PCM + C unit, the water outlet temperatures were comparatively higher than those of the PCM + C + M configuration, with a peak difference of 1.89 °C and an average difference of 0.10 °C. The average inlet water temperature was 20.43 °C, while the average outlet water temperature for the PCM + C and PCM + C + M units increased to 28.93 °C and 27.03 °C, respectively.
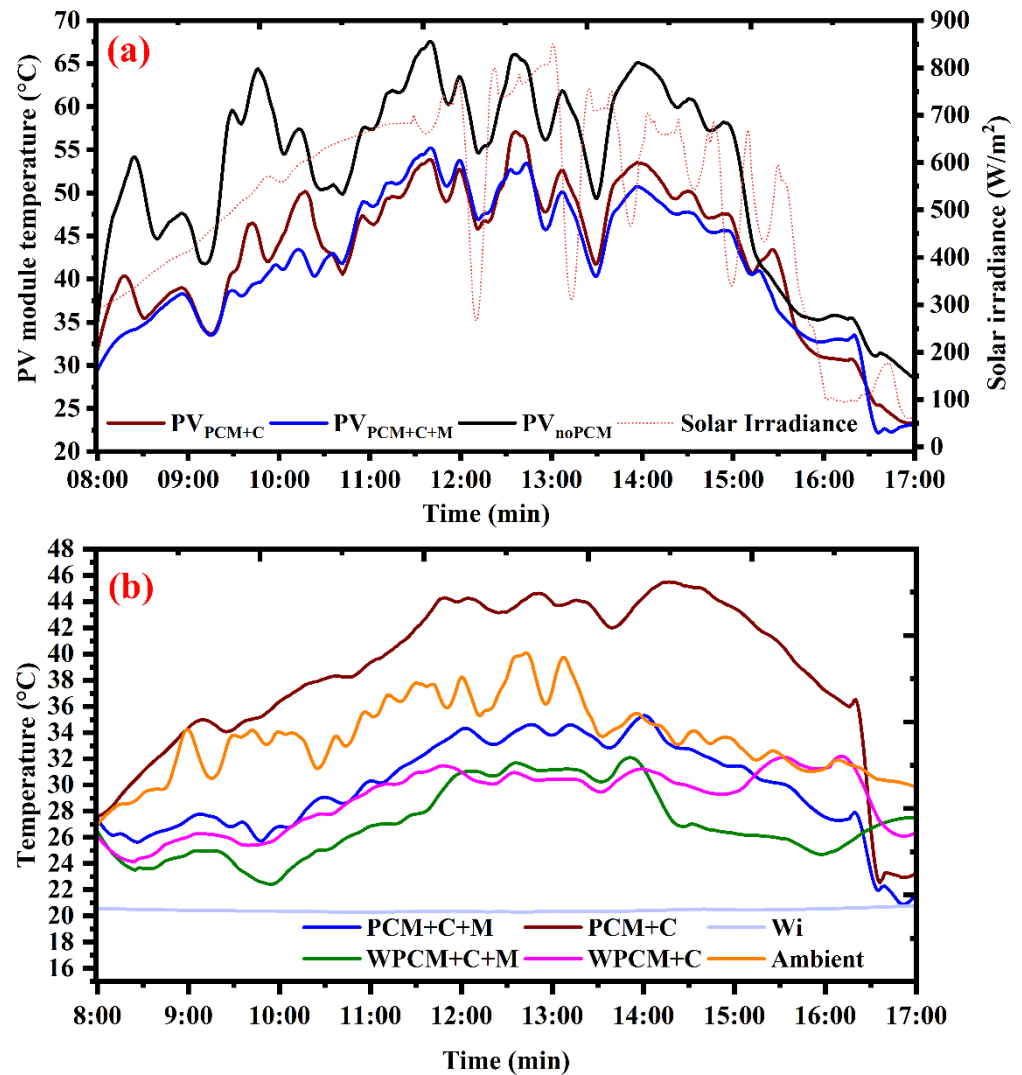
Figure 4. Thermal analysis at a constant water flow rate of 0.2 LPM: (**a**) PV module cooling performance and (**b**) heat transfer within the cooling system.

4.1.3. Water Flow at 0.4 LPM

The increased water flow inside the PCM unit effectively regulates the PV module operating temperature under all conditions. The cooling performance of the PCM + C + M-assisted PV module cooling was consistently higher throughout the experimentation period compared to the PCM + C. The average PV module operating temperatures of 46.70 °C, 38.38 °C, and 37.49 °C were recorded for PVnoPCM, PV_{PCM+C}, and $PV_{PCM+C+M}$, respectively, as shown in Figure 5a. Additionally, a water flow rate of 0.4 LPM enhanced the performance of the PCM by maintaining the backside temperatures of both PCMs at 37.47 °C and 31.84 °C, indicating that the PCMs did not completely melt. Although the PCMs remained in a semi-solid state with the effective latent heat of fusion, the cooling rates of the PV modules were comparatively lower than those observed at 0.2 LPM. The increased water flow rate improved the regulation of the PCM operating temperature more effectively than 0.2 LPM. However, the energy removed from the PCM was lower due to the limited surface area of the serpentine tube. On the other hand, the average temperature differences between the inlet and outlet water were 3.88 °C and 3.44 °C for the PCM + C and PCM + C + M, respectively, as shown in Figure 4b. Furthermore, a declining trend was observed in the outlet water temperature differences between the PCM + C and PCM + C + M, with an average and peak difference of 0.43 °C and 1.05 °C, respectively.
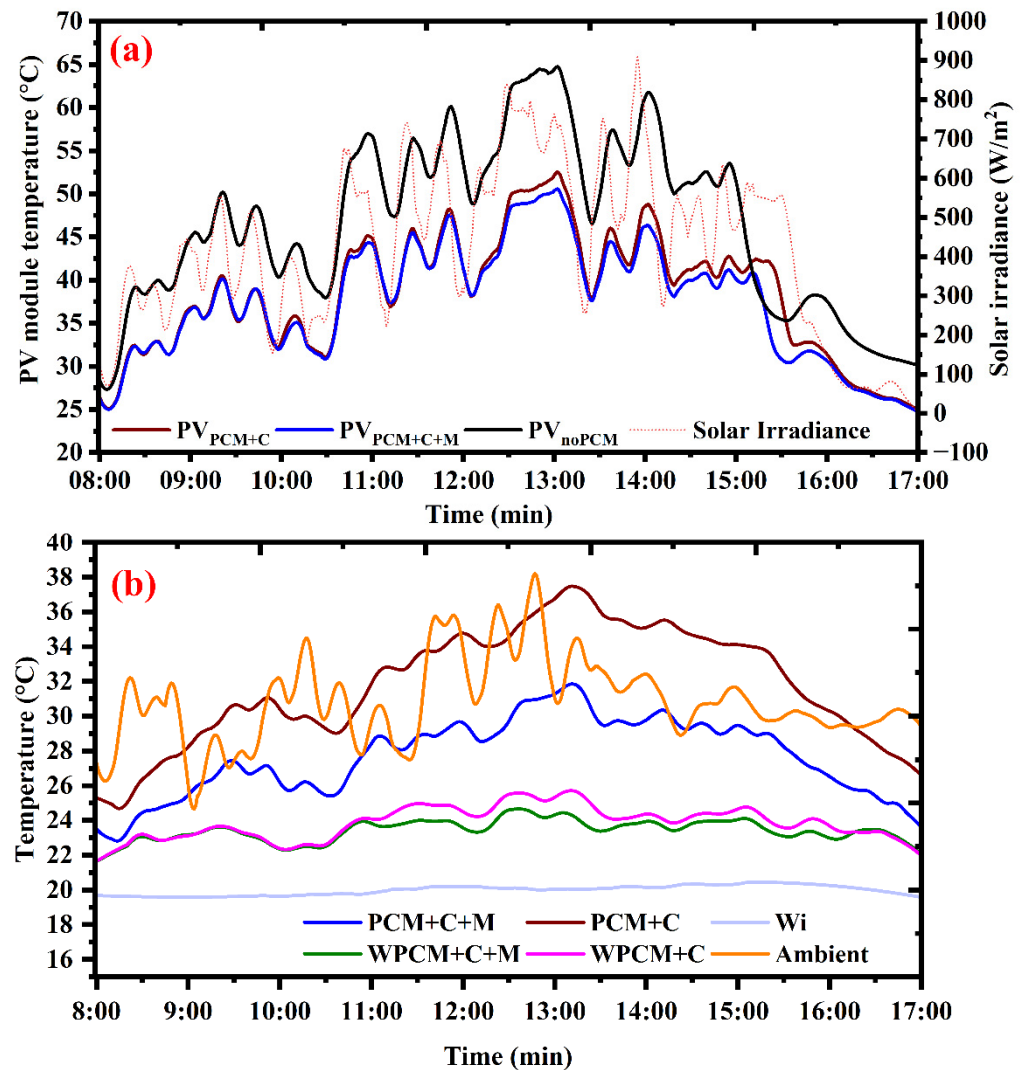
Figure 5. Thermal analysis at a constant water flow rate of 0.4 LPM: (**a**) PV module cooling performance and (**b**) heat transfer within the cooling system.

4.1.4. Water Flow at 0.6 LPM

Figure 6a shows the temperature profile of the PV module under a constant water flow of 0.6 LPM. The increase in flow rate resulted in a more pronounced difference between the operations of PCM + C and PCM + C + M in cooling the PV module. During the experimentation period, an average and peak solar irradiance of 495.24 W/m^2 and 860.51 W/m^2, respectively, were recorded. The PV$_{noPCM}$ operating temperature reached a maximum of 65.93 °C due to an elevated ambient temperature. Comparatively, the temperature difference between the water inlet and outlet was lower than at other water flow rates, as shown in Figure 6b. A notable variation in the back surface temperature of the PCM was observed, resulting in a significant temperature difference, with an average and peak of 8.78 °C and 14.57 °C for the PV$_{PCM+C}$ and 10.30 °C and 16.14 °C for the PV$_{PCM+C+M}$, respectively. The average outlet water temperature difference was 2.08 °C and 1.77 °C for the PCM + C and PCM + C + M, respectively, with a water outlet temperature difference of 0.31 °C between the PCM + C and PCM + C + M.
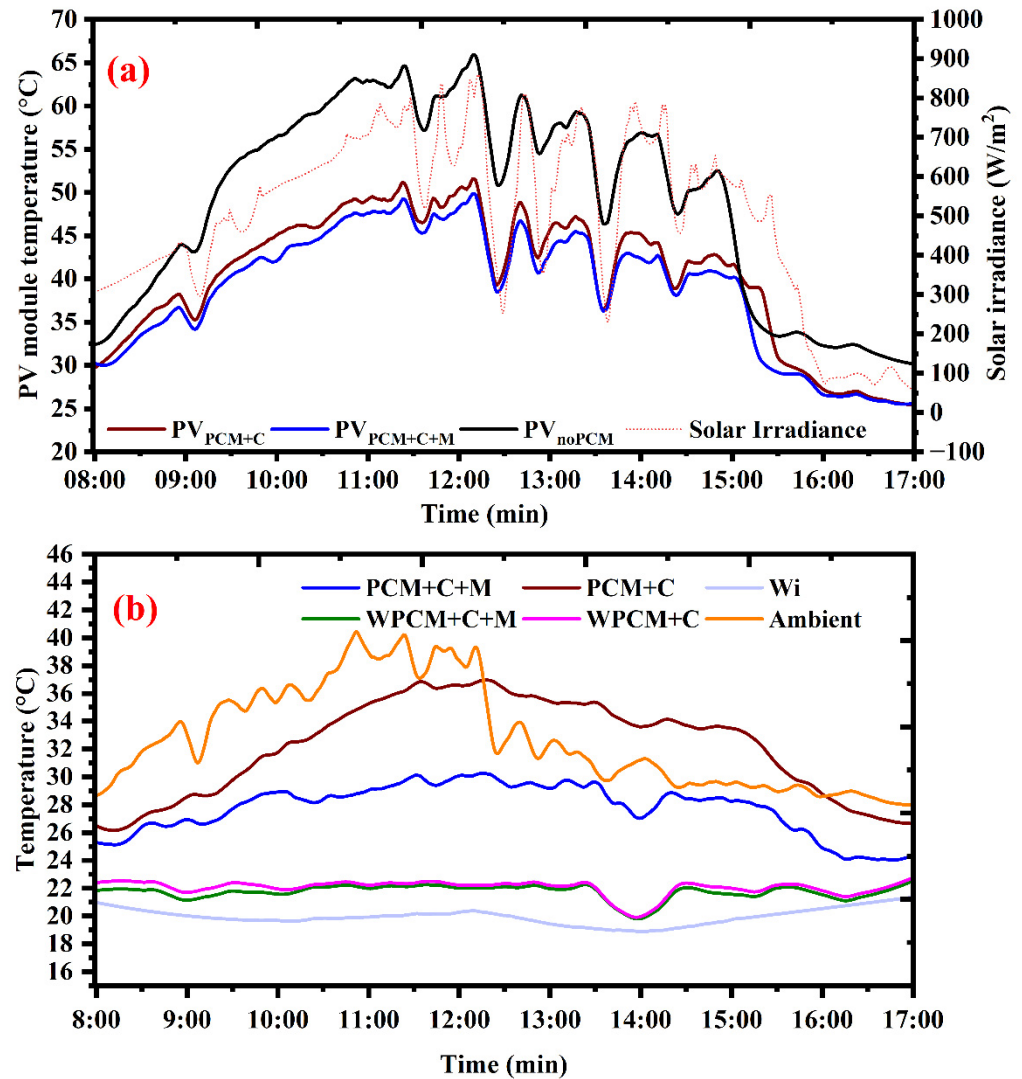
Figure 6. Thermal analysis at a constant water flow rate of 0.6 LPM: (**a**) PV module cooling performance and (**b**) heat transfer within the cooling system.

4.1.5. Water Flow at 0.8 LPM

A constant water flow rate of 0.8 LPM exhibits a similar PV module cooling trend to that observed at 0.6 LPM. The experiment was conducted under an average solar irradiance of 497.03 W/m^2, as shown in Figure 7a. The increased flow rate resulted in nearly identical temperatures for the PCM + C and PCM + C + M outlet water, as shown in Figure 7b. The average operating temperatures of the PV module for noPCM, PCM + C, and PCM + C + M were recorded as 50.29 °C, 40.81 °C, and 39.97 °C, respectively, with peak temperatures of 62.59 °C, 50 °C, and 48.72 °C, respectively.

Comparatively, the reduction in PV module operating temperature enhances the efficiency of the PV module across all cases. The temperature-corrected average PV module efficiency and corresponding temperature profiles are shown in Figure 8. Aside from the case without water flow, the PCM + C + M-assisted PV modules achieved greater efficiency enhancement than both the PCM + C and PVnoPCM. Overall, it is concluded that increasing the water flow rate helps to maintain the PCM in a mushy state for a prolonged period; however, it results in a decrease in outlet water temperature.
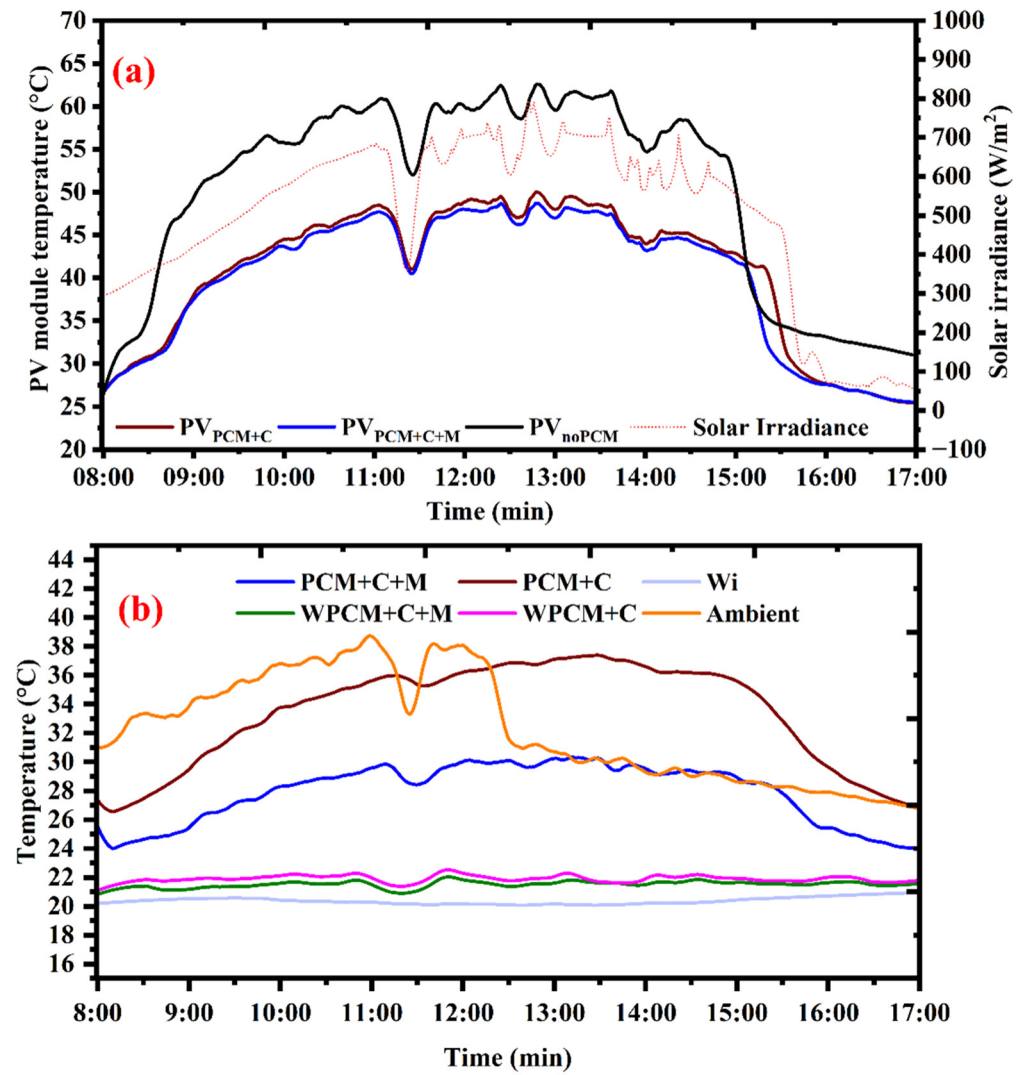
Figure 7. Thermal analysis at a constant water flow rate of 0.8 LPM: (**a**) PV module cooling performance and (**b**) heat transfer within the cooling system.
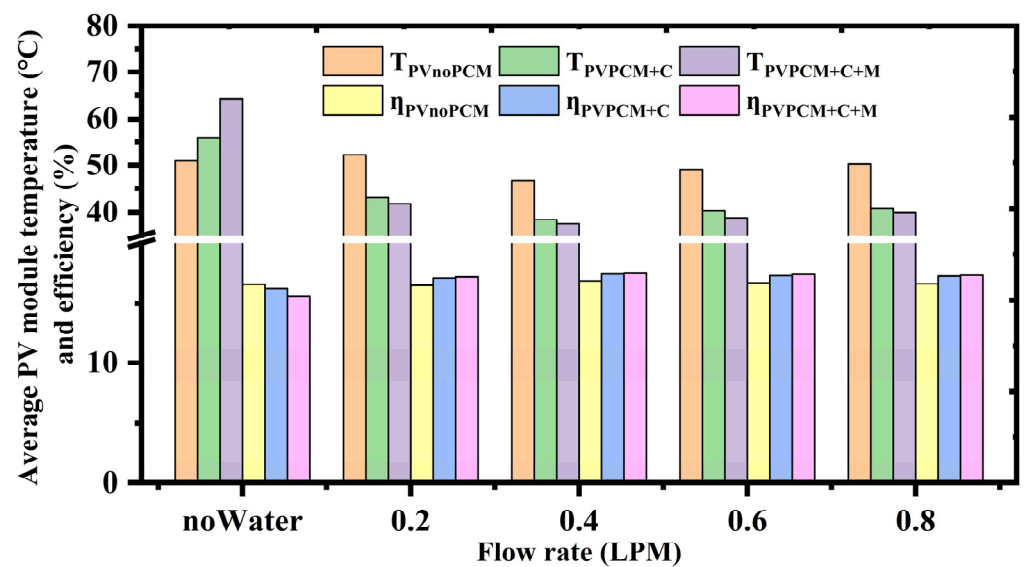

Figure 8. Average PV module temperature and temperature-corrected electrical efficiency at different flow rates.

A summary of the different flow rates and their impact on cooling the PV module is shown in Figure 9. Comparatively, a flow rate of 0.2 LPM achieved the most significant reduction in the PV module's operating temperature, with peak differences of 20.63 °C and 24.82 °C for the PCM + C and PCM + C + M, respectively. However, other water flow rates did not exhibit a similar peak cooling effect. Notably, the average cooling effect was consistent across the different flow rates (0.2, 0.4, 0.6, and 0.8 LPM), with temperature differences of 9.06 °C, 8.31 °C, 8.78 °C, and 9.47 °C for PV_{PCM+C} and 10.41 °C, 9.20 °C, 10.30 °C, and 10.31 °C for $PV_{PCM+C+M}$, respectively, on Day 1. To evaluate the consistency of the developed system, the peak and average cooling rates for selected Day 2 and Day 3 are shown in Figure 9 and Figures S1–S8. While the cooling effect varied across the experimental days, the flow rate of 0.2 LPM consistently achieved the highest cooling effect. Additionally, to assess the effectiveness of increased water flow rates, the PV module operating temperatures were normalised, as the experiments were conducted under varying operating conditions.
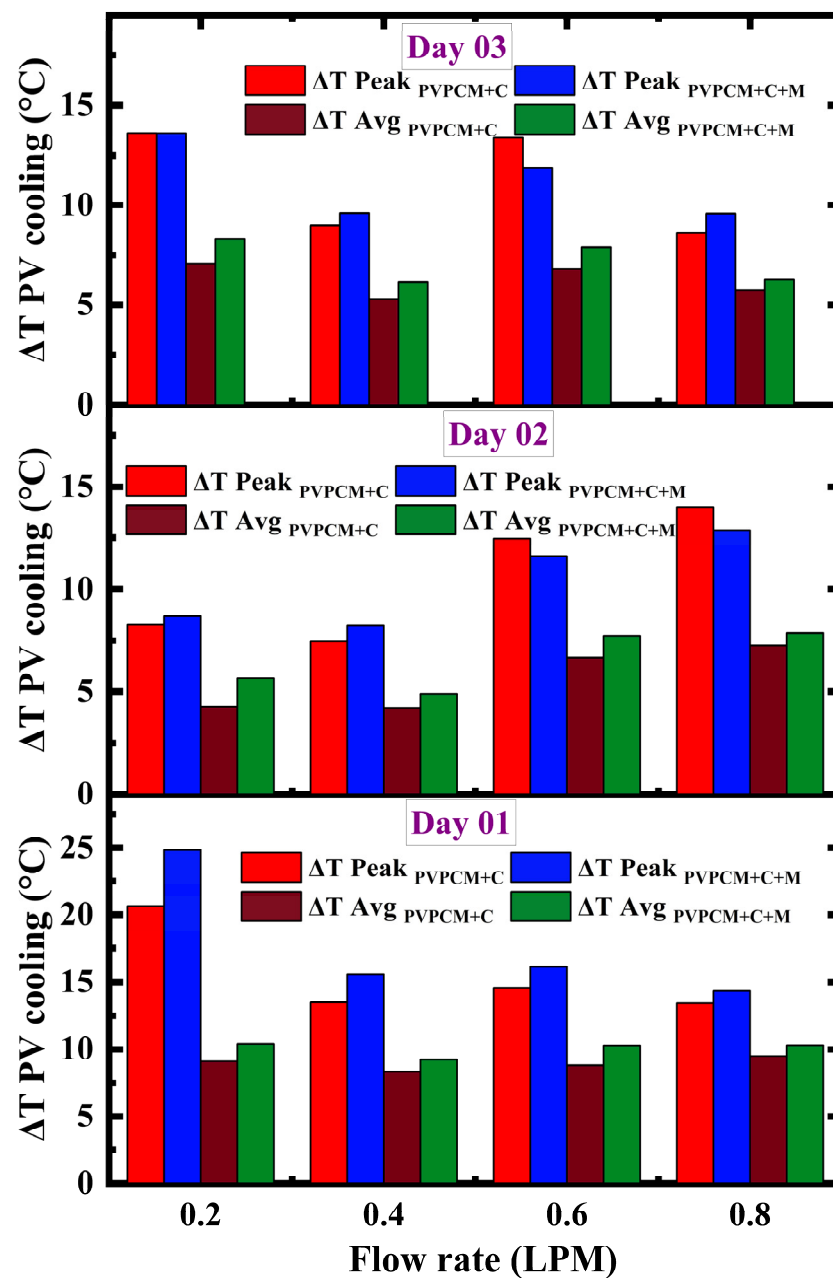

Figure 9. Reduction in PV module temperature at different water flow rates.

4.1.6. Comparative Analysis of PV$_{PCM+C}$ and PV$_{PCM+C+M}$

The reduction in PV module temperature is normalised to solar irradiance, ambient temperature, and water flow rate, as expressed in Equation (1). The experiments were conducted under outdoor conditions, where solar irradiance and ambient temperature acted as independent variables, while PV module operating temperatures were dependent on these factors. In this context, the water flow rate was considered for normalisation alongside the other two independent variables. Figure 10 shows a comparative analysis of PV module cooling under different flow rates. The lowest flow rate of 0.2 LPM demonstrated a higher cooling effect compared to other flow rates.
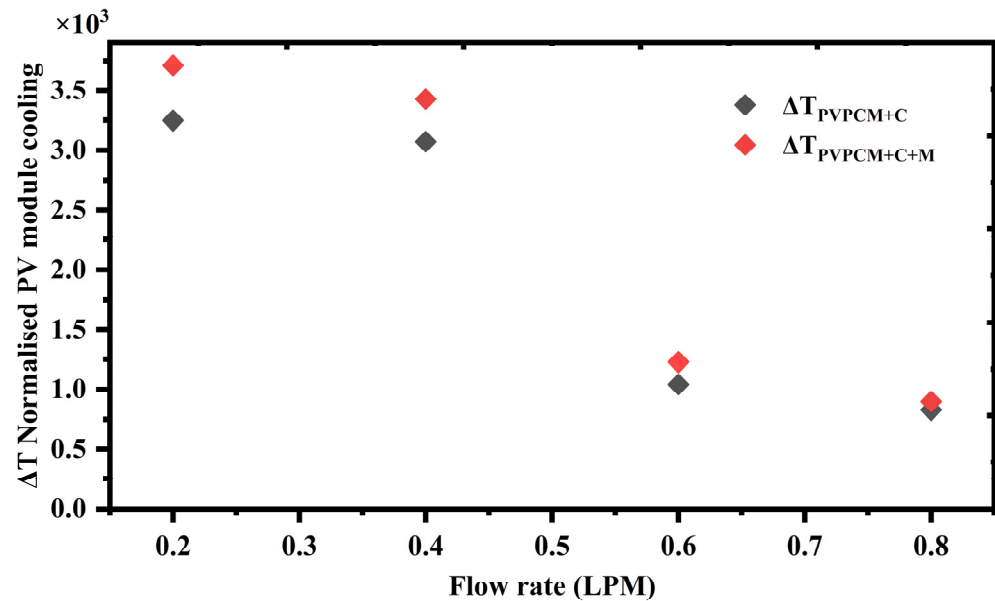

Figure 10. Normalised PV module temperature reduction for PCM + C and PCM + C + M.

Increasing the flow rate to 0.4 LPM showed a declining trend in PV module cooling performance, and further increases to 0.6 LPM and 0.8 LPM resulted in a steady-state condition. Although an increase in the water flow rate significantly reduced the PCM operating temperature, the cooling effectiveness for the PV module was lower.

An increase in the water flow rate beyond 0.2 LPM led to reduced resistance in transferring the fluid from the inlet to the outlet, resulting in less effective cooling of the PV module's operating temperatures. To achieve effective cooling at flow rates higher than 0.2 LPM, resistance in fluid motion must be enhanced, such as incorporating an intruded fin structure within the heat exchanger tube.

$$\Delta T \text{ } Normalised \text{ } PV \text{ } module \text{ } cooling = \frac{1}{n}\sum_{i=1}^{n} \frac{\Delta T_{PV},i}{G_i \times T_{AMB,i} \times HTF_i} \tag{1}$$

where ΔT_{PV} represents the cooling achieved using PCM + C and PCM + C + M, G denotes solar irradiance, T_{AMB} is ambient temperature, $HTFi$ represents the heat transfer fluid rate, i is the time interval, and n is the total number of points.

4.1.7. Comparative Analysis with Existing Systems

Table 4 presents a geographical comparison of PCM-assisted PV module cooling with the results of the presented study, including PCM + C and PCM + C + M. In Iran, a cooling effect of 20.42 °C was achieved using a PCM mass of 2 kg, while in China, a cooling effect of 19.2 °C was attained with 12.6 kg of PCM. In comparison, the developed PCM + C + M system achieved a cooling effect of 24.82 °C with only 190 g of PCM, which is the lowest

PCM quantity reported in the literature. Similarly, PCM + C achieved a cooling effect of 20.63 °C using 280 g of PCM. Although the developed system achieved a higher cooling effect, a direct comparison with the existing studies is challenging due to differences in PCM quantities and PV module capacities. To facilitate a standardised comparison, the cooling effects reported in existing studies were normalised to the 190 g of PCM used in the $PV_{PCM+C+M}$ system with the PV module capacities. This comparison is expressed as thermal cooling per 190 g of PCM and 1 Watt (TCPW). Figure 11 shows the normalised cooling effects of PV modules using different PCMs. Studies conducted in Columbia and India reported lower cooling effects, while other locations achieved moderate cooling effects. Notably, the $PV_{PCM+C+M}$ system attained the higher TCPW cooling effect of 2.482 °C, whereas PV_{PCM+C} achieved 1.399 °C. This indicates that the $PV_{PCM+C+M}$ system enhanced the cooling effect with a significantly reduced PCM quantity compared to PV_{PCM+C} and other existing models.

Table 4. Geographical comparison of PV module cooling effects with the present study.

| Location	Solar Irr (W/m^2)	Tamb (°C)	PCM Container (kg/Thickness)	PV Cooling (°C)	Reference
Iran	930	36	2 kg	12.18	[28]
Colombia	800	33	11.05 kg/2.5 cm	11.5	[26]
China	900	31.2	2 kg	12.37	[31]
Iran	826	29	2 kg	20.42	[32]
India	896	36.4	-	15	[33]
China	771	35	12.6 kg	19.2	[34]
China	1000	27	2.6 cm	10	[35]
China (Indoor)	800	28	5.27 cm	15.8	[36]
India	1100	-	65 kg	25	[37]
India	967	46.5	3.68 cm	7.8	[38]
Egypt	780	36	8 kg	8.2	[39]
Poland	1000	27–30	2–4 cm	7	[40]
France	883.45	24.09	50 kg	15.31	[41]
Thailand	850	40	190 g, 280 g	24.82, 20.63	Present study
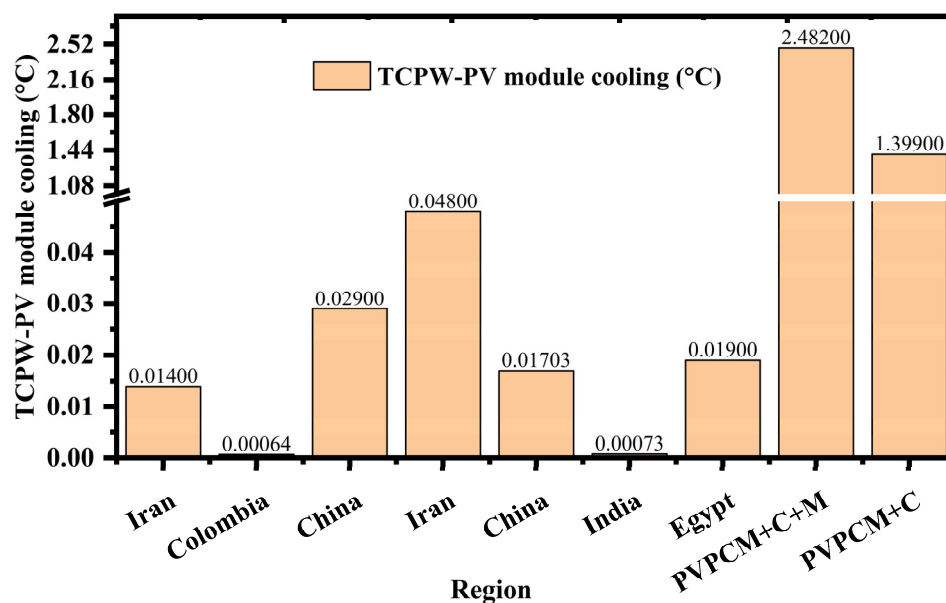
Figure 11. Comparison of the normalised PV module cooling effect per 190 g of PCM mass and PV module capacity (1 W) with existing models in the literature.

4.2. Electrical and Thermal Power Analysis

Figure 12a depicts the electrical power generation of PV modules with and without PCM. The highest power generation was recorded at 13:00 for $PV_{PCM+C+M}$, reaching 7.51 W. The corresponding power outputs for PV_{PCM+C} and PV_{noPCM} were 7.42 W and 7.11 W, respectively. $PV_{PCM+C+M}$ achieved the highest average power generation of 4.23 W, which was 0.02 W and 0.23 W higher than PV_{PCM+C} and PV_{noPCM}, respectively. Similarly, the highest thermal power was attained by $PV_{PCM+C+M}$, peaking at 151.53 W, where a water temperature difference of 10.88 °C was observed. However, PV_{PCM+C} achieved a higher average thermal power generation of 115.65 W, which was 20.76 W greater than that of $PV_{PCM+C+M}$, as shown in Figure 12b and Table 5. An increase in the water flow rate resulted in reduced thermal power, as the temperature difference between the inlet and outlet water decreased due to the lower pressure and reduced surface interaction with the PV/PCM temperatures. For a flow rate of 0.4 LPM, the average thermal powers were 50.82 W and 45.45 W for PV_{PCM+C} and $PV_{PCM+C+M}$, respectively. When the flow rate was increased to 0.6 LPM and 0.8 LPM, the average thermal powers dropped to 25.66 W and 20.94 W for PCM + C and to 21.11 W and 15.16 W for PCM + C + M, respectively. The average electrical and thermal power generations for PVnoPCM, PVPCM + C, and PVPCM + C + M are summarised in Table 5. As previously noted, increasing the water flow rate failed to enhance the cooling effect, and flow rates exceeding 0.4 LPM led to a decline in thermal power generation compared to electrical power generation. The overall combined PV_{PCM+C} electrical and thermal power generation for the PV_{PCM+C} at flow rates of 0.2 LPM, 0.4 LPM, 0.6 LPM, and 0.8 LPM were 119.86 W, 54.23 W, 29.85 W, and 25.09 W, respectively. Similarly, $PV_{PCM+C+M}$ achieved a combined power generation of 99.12 W, 48.87 W, 25.54 W, and 19.33 W, respectively. It was observed that PCM + C + M enhanced electrical power generation, while PCM + C produced a higher thermal power. In terms of combined power generation, PCM + C demonstrated superior performance compared to PCM + C + M. However, PCM + C + M utilised only 190 g of LA, representing a 47.36% reduction in PCM consumption compared to PCM + C. Considering electrical power generation, PCM + C + M is recommended due to its higher electrical power output combined with lower PCM consumption. Comparatively, the thermal power extracted by PCM + C + M would be higher if the thermal power was evaluated based on the PCM quantity used for developing a hybrid application.

Table 5. Average electrical and thermal power generation of the PV modules under different flow rates.

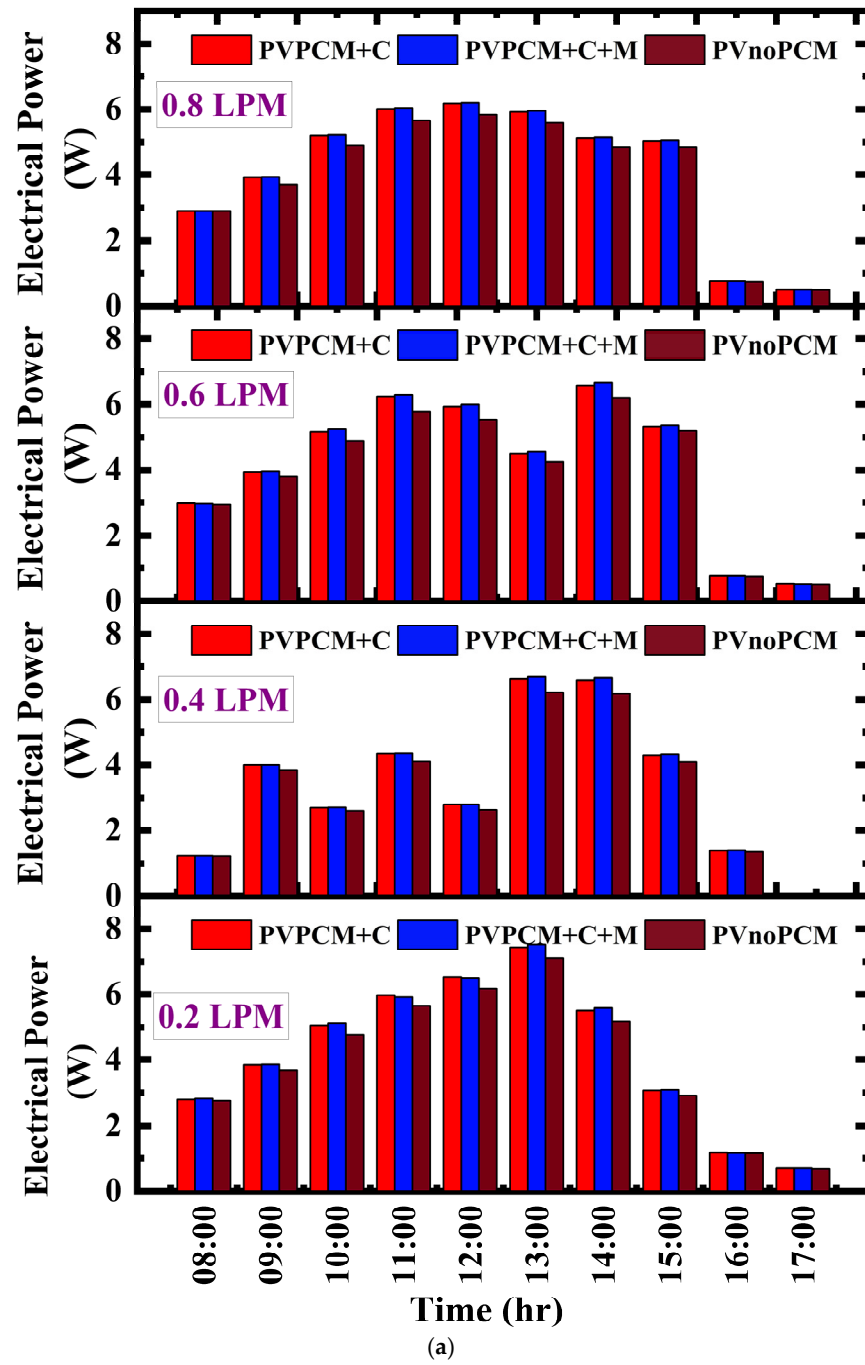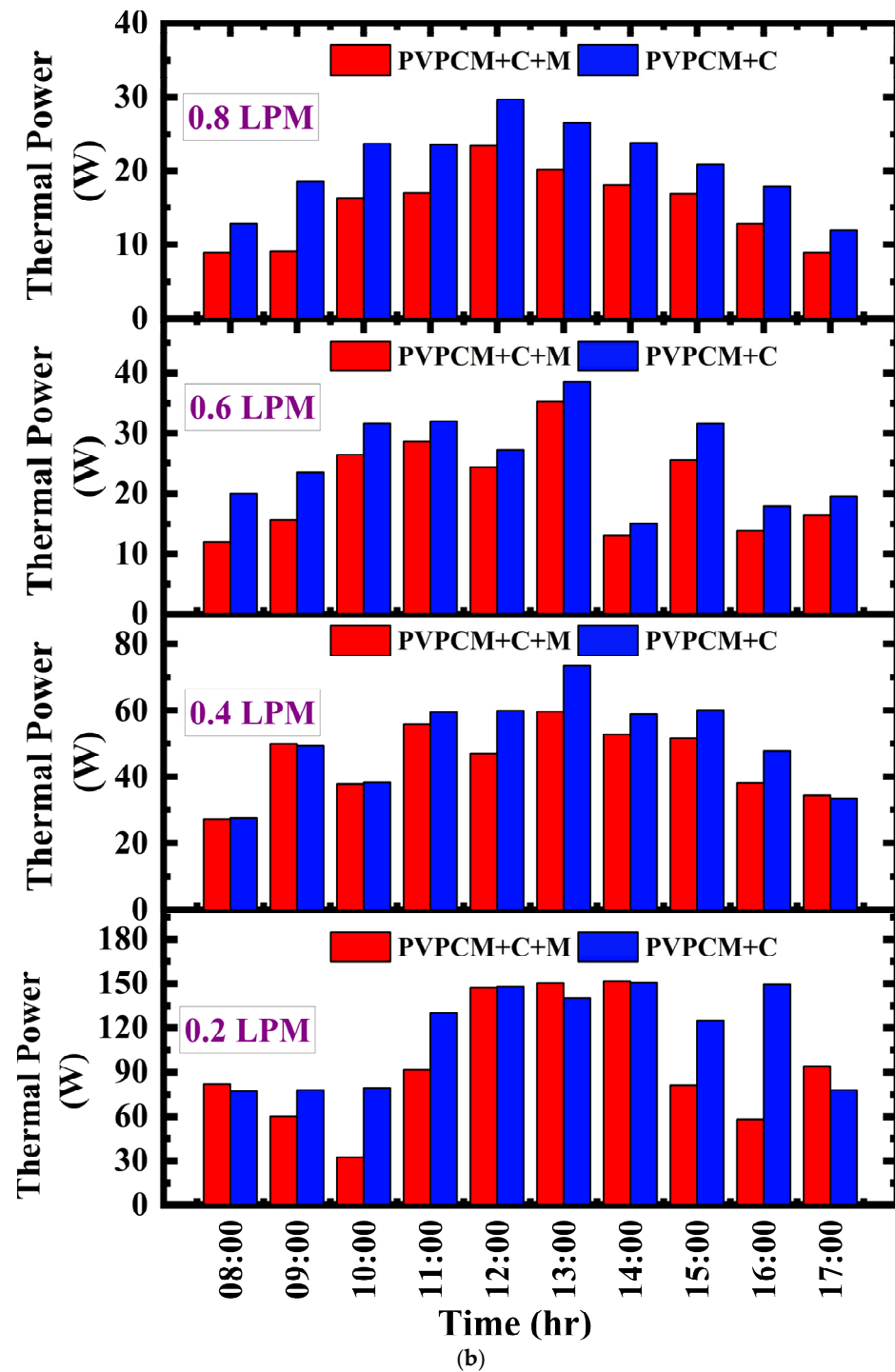| Water Flow (LPM)	Electrical Power (W)			Thermal Power (W)	
	PVnoPCM	PVPCM + C	PVPCM + C + M	PVPCM + C + M	PVPCM + C
0.2	4.005	4.205	4.225	94.897	115.653
0.4	3.228	3.406	3.425	45.445	50.824
0.6	3.984	4.192	4.23	21.105	25.663
0.8	3.948	4.152	4.167	15.162	20.939

Figure 12. *Cont.*

Figure 12. Comparison of PVPCM + C and PVPCM + C + M under different flow rates: (**a**) electrical power generation and (**b**) thermal power generation.

5. Conclusions

In this study, LA was shape-stabilised using charcoal and a charcoal combined with metal flakes to prevent liquid PCM leakage and enhance the heat transfer between the PV module and the thermal collector. The developed PV_{PCM+C} and $PV_{PCM+C+M}$ systems showed adverse effects on cooling the PV module when there was no fluid motion inside the serpentine tube, as the PCM layer thickness was 1.5 cm. Additionally, insulating the back surface of the PCM layer impeded its heat dissipation. A constant water flow rate of 0.2 LPM enhanced the heat transfer between the PV module and PCM, resulting in a

maximum cooling of 24.82 °C for PV$_{PCM+C+M}$. Conversely, an increase in water flow caused a decline in the cooling effect due to the reduced surface area of the heat pipe and water flow resistance. Higher electrical power generation was achieved with the PCM + C + M, as the addition of metal flakes to the PCM improved heat transfer between the PV/PCM and the outlet water. However, the PCM + C produced a higher outlet water temperature due to the larger PCM mass and lower thermal conductivity, which raised the PCM temperature and resulted in a higher outlet water temperature. Beyond 0.2 LPM, both electrical and thermal power enhancements were less significant, making 0.2 LPM the optimal flow rate for the developed hybrid application. It is concluded that PCM + C + M with 0.2 LPM is suitable for commercialisation due to its low PCM consumption and enhanced electrical power generation. Furthermore, it is recommended that a thermal collector with a higher surface area be developed to interact with the PV/PCM system in order to increase resistance in the water flow.

Nomenclature

Manuscript main text

PVT	Photovoltaic–thermal
PCM	Phase-change material
PCM + C	PCM with charcoal
PCM + C + M	PCM with charcoal and metal flakes
SS-PCM	Shape-stabilised PCM
TCPW	Thermal cooling 190 g of PCM and 1 Watt PV module
T$_{PV}$	PV module temperature
RT	Rubitherm
L/min	Liter per minute (LPM)
HTF	Heat transfer fluid

MWCNT	Multi-wall carbon nanotube
CuO	Copper oxide
LA	Lauric acid
LPH	Litre per hour
KPRU	Kamphaeng Phet Rajabhat University
Voc	Open circuit voltage
Isc	Short circuit current
Vmp	Voltage at maximum power
Imp	Current at maximum power
$L \times W \times D$	Length $\times$ Width $\times$ Depth
PVnoPCM	PV module without PCM
ΔT_{PV}	PV module cooling is achieved using PCM + C and PCM + C + M
G	solar irradiance
i	Time interval
n	total number of point
Figure	
T_{AMB}	Ambient temperature
T_{SKY}	Sky temperature
T_{INS}	Insulation temperature
T_{PCM}	PCM temperature
R_{AMB}	Resistance in ambient
R_{SKY}	Resistance in sky
R_{PV}	Resistance in PV module
R_{PCMU}	Resistance in PCM upper layer
R_{PCML}	Resistance in PCM lower layer
R_{INS}	Resistance in insulation
PV_{noPCM}	PV module operating temperature without PCM
PV_{PCM+C}	PV module operating temperature using PCM and charcoal
$PV_{PCM+C+M}$	PV module operating temperature using PCM, charcoal and metal flakes
PCM + C	PCM with charcoal backside temperature
PCM + C + M	PCM with charcoal and metal flakes backside temperature
WPCM + C + M	Water outlet temperature for PCM using charcoal and metal flakes-incorporated PV module
WPCM + C	Water outlet temperature for PCM using charcoal-incorporated PV module
Wi	Water inlet temperature
Ambient	Ambient temperature
ΔT PV cooling	PV module cooling difference between the PCM- and noPCM-assisted PV modules
ΔT Peak$_{PVPCM+C}$	Peak PV module cooling using PCM and charcoal
ΔT Peak$_{PVPCM+C+M}$	Peak PV module cooling using PCM, charcoal and metal flakes
ΔT Avg$_{PVPCM+C}$	Average PV module cooling using PCM and charcoal
ΔT Avg$_{PVPCM+C+M}$	Average PV module cooling using PCM, charcoal and metal flakes
TCPW-PV module cooling	PV module cooling using thermal collector 190 g of PCM and 1 Watt PV module
η	Efficiency
T	Temperature

References

1. Rekha, S.M.S.; Karthikeyan, V.; Thu Thuy, L.T.; Binh, Q.A.; Techato, K.; Kannan, V.; Roy, V.A.L.; Sukchai, S.; Velmurugan, K. Efficient heat batteries for performance boosting in solar thermal cooking module. *J. Clean. Prod.* **2021**, *324*, 129223. [CrossRef]
2. Velmurugan, K.; Karthikeyan, V.; Kumarasamy, S.; Wongwuttanasatian, T.; Sa-ngiamsak, C. Thermal mapping of photovoltaic module cooling via radiation-based phase change material matrix: A case study of a large-scale solar farm in Thailand. *J. Energy Storage* **2022**, *55*, 105805. [CrossRef]
3. Hnin, S.W.; Javed, A.; Karnjana, J.; Jeenanunta, C.; Kohda, Y. Sustainable Energy Practices in Thailand and Japan: A Comparative Analysis. *Sustainability* **2024**, *16*, 6877. [CrossRef]
4. Wongwan, W.; Pleerux, N.; Thanomsat, N.; Moukomla, S. Technical and Economic Potential of Solar Energy on Rooftops: A Case Study at Lampang Rajabhat University, Thailand. *Int. J. Geoinform.* **2024**, *20*, 82–94. [CrossRef]
5. Odeh, S.; Aden, I. Modeling of a Photovoltaic/Thermal Hybrid Panel for Residential Hot Water System. *J. Sol. Energy Eng.* **2025**, *147*, 011003. [CrossRef]
6. El Alami, Y.; Zohal, B.; Nasrin, R.; Benhmida, M.; Faize, A.; Baghaz, E. Solar thermal, photovoltaic, photovoltaic thermal, and photovoltaic thermal phase change material systems: A comprehensive reference guide. *Int. Commun. Heat Mass Transf.* **2024**, *159*, 108135. [CrossRef]
7. Rajamony, R.K.; Kalidasan, B.; Lagari, I.A.; Paw, J.K.; Sofiah, A.G.; Suraparaju, S.K.; Pandey, A.K.; Samykano, M.; Soudagar, M.E.; Khan, T.Y. Progress in research and technological developments of phase change materials integrated photovoltaic thermal systems: The allied problems and their mitigation strategies. *Sustain. Mater. Technol.* **2024**, *40*, e00921. [CrossRef]
8. Kassar, R.E.; Takash, A.A.; Faraj, J.; Khaled, M.; Ramadan, H.S. Phase change materials for enhanced photovoltaic panels performance: A comprehensive review and critical analysis. *Energy Built Environ.* **2024**. [CrossRef]
9. Tiwari, S.; Swaminathan, M.; Santhosh Eashwar, S.; Singh, D.B. Performance enhancement of the photovoltaic system with different cooling methods. *Environ. Sci. Pollut. Res.* **2022**, *29*, 45107–45130. [CrossRef] [PubMed]
10. Reji Kumar, R.; Samykano, M.; Pandey, A.K.; Kadirgama, K.; Tyagi, V.V. Phase change materials and nano-enhanced phase change materials for thermal energy storage in photovoltaic thermal systems: A futuristic approach and its technical challenges. *Renew. Sustain. Energy Rev.* **2020**, *133*, 110341. [CrossRef]
11. Teamah, H.M. A Review on Phase Change Materials Integration in Photovoltaic (PV) and Photovoltaic Thermal Systems (PVT): Scope and Challenges. *Int. Rev. Mech. Eng.* **2021**, *15*, 475–485. [CrossRef]
12. Chandrasekar, M.; Senthilkumar, T. Five decades of evolution of solar photovoltaic thermal (PVT) technology—A critical insight on review articles. *J. Clean. Prod.* **2021**, *322*, 128997. [CrossRef]
13. Laghari, I.A.; Samykano, M.; Pandey, A.K.; Kadirgama, K.; Tyagi, V.V. Advancements in PV-thermal systems with and without phase change materials as a sustainable energy solution: Energy, exergy and exergoeconomic (3E) analytic approach. *Sustain. Energy Fuels* **2020**, *4*, 4956–4987. [CrossRef]
14. Sathe, T.M.; Dhoble, A.S. A review on recent advancements in photovoltaic thermal techniques. *Renew. Sustain. Energy Rev.* **2017**, *76*, 645–672. [CrossRef]
15. Alnakeeb, M.A.; Abdel Salam, M.A.; Hassab, M.A.; El-Maghlany, W.M. Numerical study of thermal and electrical performance of a new configuration of hybrid photovoltaic solar panel phase-change material cooling system. *J. Energy Storage* **2024**, *97*, 112945. [CrossRef]
16. Almeshaal, M.A.; Altohamy, A.A. Experimental analysis of a photovoltaic thermal collector using phase change materials and copper oxide nanofluid. *J. Energy Storage* **2024**, *93*, 112265. [CrossRef]
17. Karthikeyan, V.; Sirisamphanwong, C.; Sukchai, S. Thermal investigation of paraffin wax for low-temperature application. *J. Adv. Res. Dyn. Control Syst.* **2019**, *11*, 1437–1443.
18. Karthikeyan, V.; Sirisamphanwong, C.; Sukchai, S. Investigation on thermal absorptivity of PCM matrix material for photovoltaic module temperature reduction. *Key Eng. Mater.* **2018**, *777*, 97–101. [CrossRef]
19. Elsheniti, M.B.; Zaheer, S.; Zeitoun, O.; Fouly, A.; Abdo, H.S.; Almutairi, Z. An experimental assessment of a solar PVT-PCM thermal management system in severe climatic conditions. *J. Build. Eng.* **2024**, *97*, 110691. [CrossRef]
20. Velmurugan, K.; Elavarasan, R.M.; De, P.V.; Karthikeyan, V.; Korukonda, T.B.; Dhanraj, J.A.; Emsaeng, K.; Chowdhury, M.S.; Techato, K.; El Khier, B.S.A.; et al. A Review of Heat Batteries Based PV Module Cooling—Case Studies on Performance Enhancement of Large-Scale Solar PV System. *Sustainability* **2022**, *14*, 1963. [CrossRef]
21. Velmurugan, K.; Kumarasamy, S.; Wongwuttanasatian, T.; Seithtanabutara, V. Review of PCM types and suggestions for an applicable cascaded PCM for passive PV module cooling under tropical climate conditions. *J. Clean. Prod.* **2021**, *293*, 126065. [CrossRef]
22. Waqas, A.; Jie, J. Effectiveness of Phase Change Material for Cooling of Photovoltaic Panel for Hot Climate. *J. Sol. Energy Eng.* **2018**, *140*, 041006. [CrossRef]
23. Elarga, H.; Goia, F.; Zarrella, A.; Dal Monte, A.; Benini, E. Thermal and electrical performance of an integrated PV-PCM system in double skin façades: A numerical study. *Sol. Energy* **2016**, *136*, 112–124. [CrossRef]

24. Karthikeyan, V.; Prasannaa, P.; Sathishkumar, N.; Emsaeng, K.; Sukchai, S.; Sirisamphanwong, C. Selection and preparation of suitable composite phase change material for PV module cooling. *Int. J. Emerg. Technol.* **2019**, *10*, 385–394.

25. Velmurugan, K.; Karthikeyan, V.; Sharma, K.; Korukonda, T.B.; Kannan, V.; Balasubramanian, D.; Wongwuttanasatian, T. Contactless phase change material based photovoltaic module cooling: A statistical approach by clustering and correlation algorithm. *J. Energy Storage* **2022**, *53*, 105139. [CrossRef]

26. Carmona, M.; Palacio Bastos, A.; García, J.D. Experimental evaluation of a hybrid photovoltaic and thermal solar energy collector with integrated phase change material (PVT-PCM) in comparison with a traditional photovoltaic (PV) module. *Renew. Energy* **2021**, *172*, 680–696. [CrossRef]

27. Bassam, A.M.; Sopian, K.; Ibrahim, A.; Al-Aasam, A.B.; Dayer, M. Experimental analysis of photovoltaic thermal collector (PVT) with nano PCM and micro-fins tube counterclockwise twisted tape nanofluid. *Case Stud. Therm. Eng.* **2023**, *45*, 102883. [CrossRef]

28. Naghdbishi, A.; Yazdi, M.E.; Akbari, G. Experimental investigation of the effect of multi-wall carbon nanotube—Water/glycol based nanofluids on a PVT system integrated with PCM-covered collector. *Appl. Therm. Eng.* **2020**, *178*, 115556. [CrossRef]

29. Emam, M.; Hamada, A.; Refaey, H.A.; Moawed, M.; Abdelrahman, M.A.; Rashed, M.R. Year-round experimental analysis of a water-based PVT-PCM hybrid system: Comprehensive 4E assessments. *Renew. Energy* **2024**, *226*, 120354. [CrossRef]

30. Fu, Z.; Liang, X.; Li, Y.; Li, L.; Zhu, Q. Performance improvement of a PVT system using a multilayer structural heat exchanger with PCMs. *Renew. Energy* **2021**, *169*, 308–317. [CrossRef]

31. Kazemian, A.; Taheri, A.; Sardarabadi, A.; Ma, T.; Passandideh-Fard, M.; Peng, J. Energy, exergy and environmental analysis of glazed and unglazed PVT system integrated with phase change material: An experimental approach. *Sol. Energy* **2020**, *201*, 178–189. [CrossRef]

32. Kazemian, A.; Hosseinzadeh, M.; Sardarabadi, M.; Passandideh-Fard, M. Experimental study of using both ethylene glycol and phase change material as coolant in photovoltaic thermal systems (PVT) from energy, exergy and entropy generation viewpoints. *Energy* **2018**, *162*, 210–223. [CrossRef]

33. Menon, G.S.; Murali, S.; Elias, J.; Aniesrani Delfiya, D.S.; Alfiya, P.V.; Samuel, M.P. Experimental investigations on unglazed photovoltaic-thermal (PVT) system using water and nanofluid cooling medium. *Renew. Energy* **2022**, *188*, 986–996. [CrossRef]

34. Xu, H.; Wang, N.; Zhang, C.; Qu, Z.; Karimi, F. Energy conversion performance of a PV/T-PCM system under different thermal regulation strategies. *Energy Convers. Manag.* **2021**, *229*, 113660. [CrossRef]

35. Modjinou, M.; Ji, J.; Yuan, W.; Zhou, F.; Holliday, S.; Waqas, A.; Zhao, X. Performance comparison of encapsulated PCM PV/T, microchannel heat pipe PV/T and conventional PV/T systems. *Energy* **2019**, *166*, 1249–1266. [CrossRef]

36. Yang, X.; Sun, L.; Yuan, Y.; Zhao, X.; Cao, X. Experimental investigation on performance comparison of PV/T-PCM system and PV/T system. *Renew. Energy* **2018**, *119*, 152–159. [CrossRef]

37. Preet, S.; Bhushan, B.; Mahajan, T. Experimental investigation of water based photovoltaic/thermal (PV/T) system with and without phase change material (PCM). *Sol. Energy* **2017**, *155*, 1104–1120. [CrossRef]

38. Navakrishnan, S.; Vengadesan, E.; Senthil, R.; Dhanalakshmi, S. An experimental study on simultaneous electricity and heat production from solar PV with thermal energy storage. *Energy Convers. Manag.* **2021**, *245*, 114614. [CrossRef]

39. Emara, K.; Aliwa, H.; Abdellatif, O.E.; Abd El-hameed, H.M. Experimental investigation for a hybrid aluminum oxide nanofluid-phase change material photovoltaic thermal system based on outdoor test conditions. *J. Energy Storage* **2022**, *50*, 104261. [CrossRef]

40. Klugmann-Radziemska, E.; Wcisło, P. Photovoltaic module temperature stabilization with the use of phase change materials. *Sol. Energy* **2017**, *150*, 538–545. [CrossRef]

41. Gaur, A.; Ménézo, C.; Giroux--Julien, S. Numerical studies on thermal and electrical performance of a fully wetted absorber PVT collector with PCM as a storage medium. *Renew. Energy* **2017**, *109*, 168–187. [CrossRef]

42. Gürbüz, H.; Demirtürk, S.; Akçay, H.; Topalcı, Ü. Experimental investigation on electrical power and thermal energy storage performance of a solar hybrid PV/T-PCM energy conversion system. *J. Build. Eng.* **2023**, *69*, 106271. [CrossRef]

43. IEA. Renewable Electricity Generation by Source (Non-Combustible), Thailand. 2022. Available online: https://www.iea.org/countries/thailand/renewables (accessed on 5 January 2025).

44. Karthikeyan, V.; Sirisamphanwong, C.; Sukchai, S.; Sahoo, S.K.; Wongwuttanasatian, T. Reducing PV module temperature with radiation based PV module incorporating composite phase change material. *J. Energy Storage* **2020**, *29*, 101346. [CrossRef]

45. Velmurugan, K.; Wongwuttanasatian, T. Preparation and selection of a eutectic phase change material for cooling the PV module under Thailand climatic conditions. *E3S Web Conf.* **2023**, *379*, 03004. [CrossRef]

46. Sarı, A.; Kaygusuz, K. Some fatty acids used for latent heat storage: Thermal stability and corrosion of metals with respect to thermal cycling. *Renew. Energy* **2003**, *28*, 939–948. [CrossRef]